Crop Coefficient Curve for Paddy Rice from Residual Energy Balance Calculations

A. Montazar[1]; H. Rejmanek[2]; G. Tindula[3]; C. Little[4]; T. Shapland[5]; F. Anderson[6]; G. Inglese[7]; R. Mutters[8]; B. Linquist[9]; C. A. Greer[10]; J. Hill[11]; and R. L. Snyder[12]

Abstract: The crop coefficient (K_c) values of rice paddy are important for estimating accurate rice crop evapotranspiration (ET_c), water transfers planning, efficient irrigation management, and hydrological studies. In this study, ET_c was measured and a generalized K_c curve was calculated for paddy rice in the Sacramento Valley, California. Field experiments were conducted in three rice paddy fields during the 2011–2013 growing seasons. Surface renewal analysis, after calibration using eddy covariance method, was applied to obtain sensible heat flux values from high-frequency temperature readings; latent heat flux densities were characterized by the residual of the energy balance method. The results revealed that there is considerable variability in rice water use both spatially and temporally. The average 3-year measured seasonal ET_c of the experimental fields ranged from 690 to 762 mm in Butte County and from 681 to 813 mm in the Colusa County. A mean daily seasonal ET_c of 5.3 mm d^{-1} and midseason ET_c of 5.8 mm d^{-1} was observed. The rice K_c values were lower than those commonly used to estimate rice ET_c during the midseason and were greater than expected during early growth before canopy closure. For a typical growing season of 145 days, the K_c values were estimated as 1.10, 1.00, and 0.80 for the initial-growth, midseason, and late-season stages, respectively. The generalized K_c curve is quite accurate for practical application and enables growers to determine rice crop water use in a reliable, usable, and affordable format. The proposed K_c information can be used to refine the estimates of rice consumptive water use in the Sacramento Valley for the purpose of water transfers to water-short areas of the State. These K_c values are likely applicable to other locations having similar climate to the Sacramento Valley in California. **DOI: 10.1061/(ASCE)IR.1943-4774.0001117.**

Author keywords: Crop coefficient; Energy balance approach; Evapotranspiration; Rice.

Introduction

Rice (*Oryza sativa L.*) is an important staple food crop occupying an approximate area of 158 million ha worldwide, of which approximately 50% is irrigated. California is among the top rice producing states in the United States, and more than 95% of California's rice is grown in the Sacramento Valley. Depending on market conditions, growers may be interested in fallowing rice fields and transferring water from the Sacramento Valley to water-short areas such as southern California and the San Joaquin Valley. However, this requires accurate estimates of rice crop evapotranspiration, ET_c, rather than applied water, which also includes runoff and deep percolation—neither of which are lost from the watershed and, therefore, not considered *water use*. Consequently, knowing how much applied water contributes to ET_c is crucial to determining how much water can be transferred. Accurate information on "evapotranspiration of applied water" is, therefore, needed to help water sellers and buyers to determine how much water is transferrable.

Worldwide, paddy rice is either continuously flooded or intermittently flooded and drained. Measurements of paddy rice ET_c has shown different values relative to standardized reference evapotranspiration (ET_o) as a function of the climatic conditions and cultural practices within a study area. Mohan and Arumugam (1994) found that the average daily ET_c of rice varied from less than 3.0 mm d^{-1} in the early growth period to more than 6.6 mm d^{-1} at milk stage. Tabbal et al. (2002) reported a seasonal flooded rice ET_c of 400–500 mm during wet season and 600–700 mm during the dry season in the Philippines. Other researchers found values such as 590 mm in the semiarid regions of India (Tyagi et al. 2000), 540–730 mm in the Punjab (Chahal et al. 2007), 850 mm in southern Spain (Aguilar and Borjas 2005), 700–800 mm for Mediterranean conditions in Italy (Spanu et al. 2009), and 1,440 mm in the Philippines (Alberto et al. 2011). Mean daily ET_c rates range from 4.0–5.0 mm d^{-1} for wet season (June–December) and 6.0–7.0 mm d^{-1} for dry season (January–May) in tropical areas (De Datta 1981) to 6.0 mm d^{-1} during the midseason stage (June–August) in Italy (Spanu et al. 2009). Values of 3.6–4.0 mm d^{-1} for aerobic rice fields were reported in the Philippines (Alberto et al. 2011).

[1]Project Scientist, Dept. of Plant Sciences, Univ. of California, 2242 PES Bldg., One Shields Ave., Davis, CA 95616 (corresponding author). E-mail: amontazar@ucdavis.edu

[2]Former Junior Specialist, Univ. of California, Davis, CA 95616.

[3]Former Junior Specialist, Univ. of California, Davis, CA 95616.

[4]Land and Water Use Scientist, California Dept. of Water Resources, Sacramento, CA 95814.

[5]Former Ph.D. Student, Horticulture and Agronomy Graduate Group, Univ. of California, Davis, CA 95616.

[6]Hydrologist, U.S. Geological Survey, California Water Science Center, Sacramento, CA 95819.

[7]Former Ph.D. Student Visitor, Univ. of Palermo, 90100 Palermo, Italy.

[8]Rice Farm Advisor, UCCE Butte Co., Oroville, CA 95965.

[9]Rice Specialist, UCCE at Univ. of California, Davis, CA 95616.

[10]Rice Farm Advisor, UCCE Colusa Co., Colusa, CA 95932.

[11]Rice Specialist-Emeritus, UCCE at Univ. of California, Davis, CA 95616.

[12]Biometeorology Specialist-Emeritus, UCCE at Univ. of California, Davis, CA 95616.

Note. This manuscript was submitted on December 23, 2015; approved on July 21, 2016; published online on September 23, 2016. Discussion period open until February 23, 2017; separate discussions must be submitted for individual papers. This paper is part of the ***Journal of Irrigation and Drainage Engineering***, © ASCE, ISSN 0733-9437.

The K_c values of rice, as suggested by the Food and Agricultural Organization of the United Nations (FAO 1977), are used widely where localized ET_o estimates are available. In many irrigation areas, however, K_c values are not available. Allen et al. (1998) suggested that the crop coefficient values need to be derived empirically for each crop based on lysimeteric data and local climatic conditions. Reuss (1980) reported rice K_c values for tropical Pakistan climate conditions, which were greater than those values given by FAO. Multiseasonal empirical crop coefficients for lowland rice were developed using the meteorological and lysimetric data by Mohan and Arumugam (1994). They estimated the K_c values for rice at the four crop growth stages (initial growth, crop development, reproductive, and maturity) were 1.15, 1.23, 1.14, and 1.02, respectively. Allen et al. (1998) recommended 1.05, 1.20, and 0.90–0.60 for continuously flooded paddy rice during the initial-growth, midseason, and late-season stages, respectively. Seung Hwan et al. (2006) reported K_c values between 0.78 and 1.58 during the midseason stage (March–May) for a region of Korea with total growing season lengths of 100–110 days. A mean K_c value of 0.9–1.07 was proposed during 140 days growing season, sowing to maturity, in the Sardinia region of Italy (Spanu et al. 2009). Alberto et al. (2011) reported an average K_c value of 0.95, 1.0, and 0.97 for the vegetative, reproductive, and ripening stages, respectively. Lourence and Pruitt (1971) obtained monthly K_c values in the range of 1.02–1.05 based on the Bowen ratio method for rice grown in California.

Seasonal rice evapotranspiration and mean daily ET_c were determined as 750–800 mm and 5.2 mm d^{-1}, respectively, for sprinkler-irrigated rice in a semiarid region of Spain (Moratiel and Martínez–Cob 2013). The crop coefficients for the initial-growth, midseason, and late-season stages were reported to be 0.92, 1.06, and 1.03, respectively. The total growing season was between 150 and 160 days. Lal et al. (2012) estimated 835 mm as the seasonal ET_c of rice paddy fields in the Sacramento Valley using the remote sensing based on the surface energy balance algorithm for land (SEBAL) method. The K_c values of 1.17 and 0.85 were reported for June and September by these researchers for rice paddies of the area. The K_c and water-use values in California were reported slightly lower in the dry-seeded rice system compared with the water-seeded rice system (Linquist et al. 2015).

Based on older literature, ET_c in California rice cultivation ranges from 914 to 1,158 mm (California Department of Water Resources 1998). However, the methods to determine ET_o and ET_c, in addition to the morphology of the rice plants, has changed considerably since the earlier K_c values were reported (Lourence and Pruitt 1971). Clearly, the K_c estimates for the rice paddy fields, specific to California, need updating for use in estimating rice ET_c for water transfers. Carefully developed K_c information along with accurate ET_o values can provide robust and accurate ET_c estimates. The present study aims to determine the rice ET_c using the residual of the energy balance method over rice in the Sacramento Valley, California, to develop a typical seasonal crop coefficient curve.

Surface Renewal Technique

A wide range of measurement techniques have been developed for measuring either ET or its components. Each of these techniques is representative within a spatial and temporal scale. Results must be extrapolated for specifying ET rates outside of these scales. Allen et al. (2011) categorized three main approaches for ET measurements, which include methods related to the energy balance (e.g., Bowen ratio or residual of the energy balance), methods related to mass balance (e.g., lysimeters), and independent methods [e.g., latent heat flux from an eddy covariance (EC) system]. The surface renewal (SR) method is used to estimate the sensible heat flux density (H) and the latent heat flux density (LE) as the residual of the energy balance (REB) using LE = R_n–G–H, in which R_n is the net radiation and G is the ground heat flux density at the soil surface. Another energy balance approach is to determine H from a sonic anemometer with EC calculations, and again determine LE as the REB. Thus, both the EC and SR methods were proposed for estimating H and calculating LE using the REB approach (Paw U et al. 1995; Paw U et al. 2005). More details on the SR and EC methods may be found in Paw U and Brunet (1991), Paw U et al. (1995, 2005), Snyder et al. (1996), Spano et al. (1997), Massman and Lee (2002), and Shapland et al. (2013). Measuring sensible heat flux with the EC method using a sonic anemometer was described in Lee et al. (2004) and Shaw and Snyder (2003).

A paper by Zapata and Martínez-Cob (2002) compared the REB method, with H from SR, with the lysimeter measurements of ET_c of wheat, and they found that the REB method slightly underestimated the lysimeter ET_c. A root mean square error (RMSE) $\approx$ 1.0 mm d^{-1} was reported. However, the researchers used an $\alpha = 1.0$ calibration factor from the literature rather than calibrating the SR measurements of H against the sonic anemometer H. Field calibration of the SR method might have improved the estimates of lysimeter ET_c. Another paper by Moratiel and Martínez-Cob (2013) compared the REB method and lysimeter measurements of upland rice ET_c. They reported a mean REB to lysimeter ET_c ratio of 0.96 and a RMSE $\approx$ 0.75 mm d^{-1}. Therefore, the ET_c from the REB method was approximately 4% less than from the lysimeter. In their experiment, they found α calibration factors by comparing the SR and EC measurements of H.

Although the lack of closure in EC measurements has not been resolved in the literature, Castellvi et al. (2008) reported good closure for energy balance measurements when both H and LE were computed using the SR method. This implies that the REB method with SR-estimated H should give good results, assuming that R_n, G, and H are accurately determined. Because the calibrated $\alpha H'$ from SR gives good estimates of H from EC, the REB method using H from EC should also provide good estimates of LE.

The use of H estimated from SR analysis in conjunction with measured net radiation and ground heat flux density can provide an easily transportable and relatively inexpensive method to estimate LE. The SR method uses high-frequency temperature measurements from fine wire thermocouples to determine an average change in temperature with time within the air above a canopy, and the volumetric heat content of the air to estimate H. The SR method is based on conservation of energy with a strong theoretical basis. However, an empirical calibration factor was required to estimate sonic H from the SR measurements during the early research. The SR calibration factor for a particular canopy and measurement height is found by determining the slope of a linear regression through the origin of half-hourly EC H, a RMSE $\approx$ 0.75 mm d^{-1}, versus the uncalibrated SR sensible heat flux (H'). In fact, the SR H is calculated from the average heating of the air parcel and the number of times the air parcel is renewed at the surface over 30-min intervals as follows:

$$H_{SR} = \alpha H' = \alpha \left[z \rho C_p \left(\frac{a}{t_r} \right) \right] \quad (1)$$

where α = calibration factor; z = measurement height; ρ = air density (g m^{-3}); C_p = specific heat of air at constant pressure (J g^{-1} K^{-1}); and a = average ramp amplitude (K), which corresponds to the temperature enhancement of the air parcel. t_r is the

mean air parcel renewal time over the sampling period (Paw U et al. 1995).

The ramp amplitude (a) and duration (t_r) were determined using the Van Atta ramp model (Van Atta 1977), which uses half-hour means of the second, third, and fifth moments of the air temperature structure function [Eq. (2)]

$$S^n(r) = \frac{1}{m-j}\sum_{i=1+j}^{m}(T_i - T_{i-j})^n \quad (2)$$

where m = number of data points in the half-hour interval measured at frequency (f); n = order of the structure function; j = sample lag between data points corresponding to a time lag ($r = j/f$); and $T_i = i$th temperature sample (K). In this research, the second, third, and fifth moments were calculated and recorded for both $r = 0.25$ s and $r = 0.50$ s. Uncalibrated H values (H') were calculated separately for each time lag from the mean ramp amplitude and mean ramp period [Eq. (1)].

There are many studies on the use of the SR method for estimating evapotranspiration, including Snyder et al. (1996), Spano et al. (1997), Anandakumar (1999), Zapata and Martínez-Cob (2002), Consoli et al. (2005), Castellví et al. (2006), Snyder and O'Connell (2007), Castellví et al. (2008), Drexler et al. (2008), Snyder et al. (2008), Spanu et al. (2009), Castellví and Snyder (2009), Castellví and Snyder (2010), Moratiel and Martínez-Cob (2012), Castellví et al. (2012), Shapland et al. (2012b), Suvočarev et al. (2013), Rosa et al. (2013), Moratiel and Martínez-Cob (2013), and Snyder et al. (2015). A detailed explanation of the current methodology may be found in Shapland et al. (2013).

Research on use of the SR method without the need for calibration was reported by Castellví et al. (2006) and Shapland et al. (2014). Castellví et al. (2006) combined similarity theory with the SR method to attempt to find accurate estimates of H without the need for calibration against sonic anemometer data. Shapland et al. (2014) found that the need for calibration mostly results from the use of thermocouple wire diameters that are too large, and hence too much thermal mass. Most early SR research employed 76.2-μm diameter fine wire thermocouples, primarily because they are less likely to break than smaller diameter thermocouples. Recent research has shown that self-calibration of the SR method is possible if corrections are made for the wire diameter (Shapland et al. 2014). The least-expensive sonic anemometer is more than 300 times more expensive than a thermocouple for measuring SR H', and thermocouples can be mounted just above the canopy top so the difference between the measurement height and the zero-plane displacement is smaller than for a sonic anemometer, which should be mounted at a height of at least 1.4 times the maximum canopy height. For the SR method, the fetch ratio is approximately 10:1, and for a sonic anemometer, the minimum fetch requirement is approximately 50:1. Therefore, the fetch requirement for a thermocouple to measure H using SR is much less than for a sonic anemometer to measure H with EC. In addition, thermocouples are much simpler to mount, move, and monitor than a sonic anemometer.

Materials and Methods

Experimental Fields

The experimental fields were chosen at the Sacramento Valley, California, which has mild winters, and hot and dry summers. The natural levees that border the Sacramento-Feather River system create backwater basins of heavy clay soils that are highly suitable to rice production. The amount of land annually farmed in rice is influenced by factors such as market conditions, weather, and drought water bank agreements. The total rice area of the Valley identified by USDA in 2009 was 220,600 ha (USDA 2011).

Field experiments were conducted in three rice paddy fields during three growing seasons of 2011 through 2013 in the Sacramento Valley. Only the rice variety that is most commonly grown for rice production in the study area, M-206, was studied. M-206 is a very early maturing, semidwarf, glabrous, Calrose quality, and medium-grain.

The locations and the information of the experimental rice paddies are provided in Table 1. In 2011–2012, the "east" rice research field was located 0.8 km straight west of the south end of the Thermalito Afterbay (4.5 km north–northeast of Biggs). In 2013, the research field was moved approximately 4.5 km due north to a field just south of the Richvale Highway (4 km east of Richvale). In 2011–2012, the north field was located just east of Z-Road, approximately 5 km north of Highway 162. The intersection of Z-Road and Highway 162 is 5.25 km east of Butte City. In 2013, the North station was moved to a field 7.4 km north–northeast of Nelson. The south research field was located 4.25 km northeast of Williams (approximately 2.5 km south of Highway 20).

Climate data from the California Irrigation Management Information System (CIMIS) Colusa #32 station are presented in Table 2 as an example of the climate in the Sacramento Valley. Data from the CIMIS network are available at http://www.cimis.water.ca.gov. The CIMIS weather station network (Snyder and Pruitt 1992) was established in 1982 by California Department of Water Resources and University of California at Davis to provide reference ET (ET_o) information for growers and urban irrigators in managing their water resources more efficiently. The CIMIS Colusa #32 station was activated on January 13, 1983, and it is still active. The station is located in Colusa County at elevation 12.2 m, latitude 39°13′37″ N, and longitude 122°1′28″ W. The cumulative ET_o from May to September, which is the main growing season for rice paddies in the area, is approximately 850 mm (Table 2). The *annual average*

Table 1. Field Number, Study Season, Experimental Site, Nearby Town, Latitude, Longitude, and Elevation for the Rice Research Fields

Field identifier number	Study season	Experimental site	Nearby town	County	Latitude (N)	Longitude (W)	Elevation (m asl)
E11	2011	East (wet)	Biggs	Butte	39°26′46.6″	121°42′25.1″	25.0
E12	2012	East (wet)	Biggs	Butte	39°26′46.6″	121°42′25.1″	25.0
E13	2013	East (wet)	Richvale	Butte	39°29′33.0″	121°41′52.0″	35.7
N11	2011	North (wet)	Butte City	Butte	39°30′32.5″	121°05′23.9″	31.7
N12	2012	North (wet)	Butte City	Butte	39°30′32.5″	121°05′23.9″	31.7
N13	2013	North (wet)	Nelson	Butte	39°36′58.7″	121°44′25.5″	45.4
S11	2011	South (wet)	Williams	Colusa	39°10′11.4″	122°06′10.1″	14.3
S12	2012	South (wet)	Williams	Colusa	39°10′11.4″	122°06′10.1″	14.3
S13	2013	South (wet)	Williams	Colusa	39°10′11.4″	122°06′10.1″	14.3

Note: m asl = meters above mean sea level.

Table 2. Monthly Mean Climate Data for Colusa #32 CIMIS Station

Month	Rain (mm)	Solar radiation ($MJ\,m^{-2}\,d^{-1}$)	Maximum air temperature (°C)	Minimum air temperature (°C)	Mean air temperature (°C)	Dew point temperature (°C)	Mean wind speed ($m\,s^{-1}$)	Total ET_o (mm)
January	82.5	77.4	12.9	2.7	7.3	4.7	2.2	29.9
February	77.1	124.7	16.2	3.8	9.7	5.6	2.4	49.5
March	55.2	183.6	19.4	5.7	12.4	6.9	2.5	86.6
April	21.8	243.2	23.0	7.2	15.2	7.2	2.4	131.8
May	19.4	292.0	27.4	10.8	19.4	9.8	2.4	168.9
June	7.6	324.4	31.3	13.9	22.8	12.3	2.3	179.3
July	0.9	325.4	34.2	15.5	25.2	14.2	2.2	200.8
August	1.9	291.1	33.8	14.2	24.1	12.8	2.1	170.4
September	8.1	232.9	31.6	11.7	21.4	11.1	2.0	130.5
October	20.3	164.7	26.1	8.2	16.6	7.8	2.0	92.7
November	50.1	101.8	18.1	4.6	10.9	5.9	2.0	46.6
December	55.9	73.8	12.7	1.9	6.9	3.6	2.2	31.1

temperature and total *precipitation* of the area are 16 and 400 mm, respectively.

Instrumentation

In the experiments, the NR LITE net radiometer from Kipp & Zonen (Delft, Netherlands) was used to measure net radiation. Soil (and water) heat storage and fluxes were measured with one REBS HFT3 heat flux plate inserted at 0.05-m depth below the soil surface, and soil and water temperature measured at three depths above the heat flux plates using 107 thermistor (temperature) probes from Campbell Scientific (Logan, Utah). The first thermistor was inserted horizontally at approximately 0.025 m below the soil surface. The other two thermistors were mounted on a length of PVC pipe with a hinge on the bottom. There was a floating device attached to the top of the PVC pipe, and the combination of the hinge and float allowed the pipe and sensors to move up and down with the water level, so that the soil and water temperatures were always recorded just below the soil surface, about halfway between the soil and water surfaces, and just below the water surface. The probe just below the water surface was mostly shaded from direct sunlight by the PVC pipe. Global Water Instrumentation WL400 water level recorders (Rancho Cordova, California) were used to continuously measure the depth of water to determine the volume of water above the ground, to allow for calculation of the volumetric heat capacity of the saturated soil and water above the heat flux plates. In 2013, the setup for the water level recorder was changed because sunlight was damaging the plastic coating of the water level recorder cable. To solve this problem, the water level recorder and cable were laid on the ground, and the tip of the water level recorder was place inside a horizontal PVC pipe that was staked to the ground. There was a screen over the ends of the PVC pipe to minimize entry of soil sediment.

High-frequency temperature data for the SR estimates of H were measured with a 76.2-μm diameter Chromel-Constantan thermocouple model FW3 from Campbell Scientific. RM Young Model 81000RE three-dimensional sonic anemometers (Traverse City, Michigan) were used to collect high-frequency wind velocities in three orthogonal directions at 10 Hz to estimate H using the EC technique.

The water level was recorded in all fields during the experiments, but there were missing data, as a result of sensor problems, during early growth in the first two years. The water-level data were more complete in 2013.

All data were recorded using Campbell Scientific CR3000 data loggers. The fine-wire thermocouple data and sonic anemometer data were collected at a 10-Hz sampling rate, and the other variables were sampled once per minute. Half hourly data were archived for later analysis. All of these instruments were set up over a flux station in each of the experimental fields.

Flux Data Processing

Rice ET_c was measured using the REB. The available energy components, R_n and G, were measured, and both the EC and SR techniques were employed to determine H. The latent heat flux density was estimated as $L = R_n - G - H$.

A time lag of 0.5 s was used to compute uncalibrated half-hourly SR sensible heat flux density (H') using a modified version of the Van Atta (1977) structure function. The modified version is described in Shapland et al. (2014). The modification was unavailable during the project, but all of the data were reanalyzed using the modification in 2014. This decreased the number of missing half-hourly data that are often observed during stable atmospheric conditions. After obtaining the half-hourly H' data, a calibration (α) factor was determined by computing the slope through the origin of H from the EC versus H' from the SR. Finally, the calibrated SR value for H was estimated as $H = \alpha H'$. The EC H was preferentially used over the SR H', but $\alpha H'$ was used when the EC data were missing. The advantage from using both the EC and SR methods is that they are independent, and similar results provide a high level of confidence in the data.

Sonic anemometer data were collected and analyzed following Lee et al. (2004), using half-hourly calculation intervals. The high-frequency wind velocities from the sonic anemometer were rotated into the natural wind coordinate system using the first and second rotation algorithms. Sensible heat flux density was calculated from the product of the air density, the specific heat of air, and the covariance of the vertical wind and the virtual sonic temperature. The Webb-Pearman-Leuning (WPL) corrections were applied to the sensible heat flux densities (Webb et al. 1980).

After determining the latent heat flux density, the ET_c in $mm\,d^{-1}$ was calculated by dividing the LE in $MJ\,m^{-2}\,d^{-1}$ by $L = 2.45\ MJ\,kg^{-1}$ to obtain the ET_c in $kg\,m^{-2}\,d^{-1}$, which is equivalent to $mm\,d^{-1}$.

In some cases, there were missing data for a period of time because of instrumentation or battery problems. For short periods, i.e., less than 3 h, the values were estimated using a linear trend between observed points. This happened primarily because of weak batteries during nighttime when the ET_c rates were low and a linear interpolation was reasonable. In a few cases, data were missing much of the night and the data from the previous night were substituted if there was no reason to expect changes.

Identifying the Growth Dates

Crop coefficient curves are often subjectively determined by trying to match a plot of observed data versus time with a hand-drawn approximation. This is done primarily because there is considerable scatter in all measured ET data. In this study, an attempt was made to be less subjective, and the observed solar and net radiation balance over the rice crop was used to identify inflection points in the K_c curve using data from the three rice fields in 2013 when there were few missing data. Daily solar radiation at each experimental field was derived from data provided by spatial CIMIS (http://www.cimis.water.ca.gov/SpatialData.aspx). To generate daily solar radiation, spatial CIMIS uses the visible band of the National Oceanic and Atmospheric Administration's (NOAA) Geostationary Operational Environmental Satellite (GOES) and Heliosat-II model. A combination of data acquired from this process and interpolated from CIMIS station measurements is used to estimate solar radiation at a 2-km spatial resolution.

The same linear approach was applied to identify segments of the K_c curve corresponding to initial-growth, rapid, midseason, and late-season growth periods, as was implemented in FAO 24 (Doorenbos and Pruitt 1977) and FAO 56 (Allen et al. 1998). Daily solar and net radiation data were filtered by eliminating that day of data when the difference from the mean value for the following 5 days exceeded 5%. This eliminated major spikes from the data. Then, the ratio of R_n/R_s was computed and linear interpolations between estimated inflection points were subjectively determined to fit the plotted data.

Identifying Crop Coefficients during the Growing Season

Using the first flood date and ending date (harvest) for the nine experimental fields, the intermediate growth (inflection point) dates were computed using the percentages of the season. On each day of the season, the predicted ET_c ($ET_{c(p)}$) was estimated as

$$ET_{c(p)} = ET_o \cdot K_c \tag{3}$$

where ET_o = standardized reference evapotranspiration for short canopies from spatial CIMIS (Hart et al. 2009) for the coordinates of the experimental fields. The seasonal K_c curve was determined for each of the experimental fields by varying K_{c1} (initial-growth K_c), K_{c2} (midseason K_c), and K_{c3} (the K_c on Date E) until the RMSE of the daily predicted $ET_{c(p)}$ versus the daily observed ET_c ($ET_{c(o)}$) was minimized. The RMSE is calculated as

$$\text{RMSE} = \sqrt{\frac{\sum_{i=1}^{n} (ET_{ci(p)} - ET_{ci(o)})^2}{n}} \tag{4}$$

where the subscript i indicates the ith day of n pairs of predicted and observed data (Tsay 2005). The RMSE was calculated separately for each of the three experimental fields per year for the 2011–2013 experimental fields. A RMSE over all of the fields and years was also computed. The overall RMSE was used to identify the optimal crop coefficients. Finally, the seasonal total $ET_{c(p)}$ and $ET_{c(o)}$ were determined for each of the experimental fields. On days when there were missing $ET_{c(o)}$ data, the $ET_{c(p)}$ value was substituted on that date. Using the seasonal total $ET_{c(p)}$ and $ET_{c(o)}$ from the nine experimental fields, the RMSE was determined. The normalized root mean square error (NRMSE) of the comparisons is also reported as the ratio of RMSE to the mean of the observed data (Tsay 2005). The daily $ET_{c(p)}$ and $ET_{c(o)}$ data were again compared using the RMSE for all experimental field and year combinations. In addition, the seasonal $ET_{c(p)}$ and seasonal $ET_{c(o)}$ data were computed and compared.

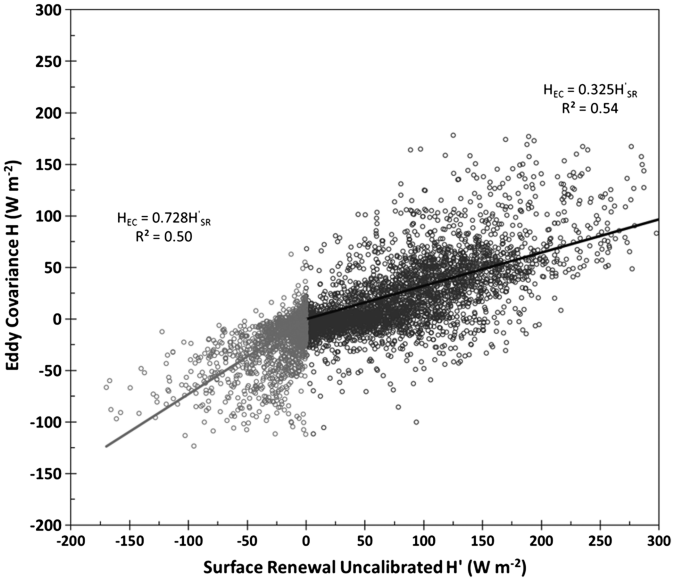

Fig. 1. Half-hourly sonic anemometer EC H versus uncalibrated SR H' from data collected at the east rice field station during 2012 (E12)

Results

Quality Assurance of Flux Density Data

The SR calibration factors were derived at each experimental field for each of the three seasons. As in earlier experiments, the calibration factors were different under stable and unstable atmospheric conditions, so the SR calibration factors were determined separately for positive and negative H' values (Shapland et al. 2012a). The results from the calibration process of the east rice paddy field from 2012 (E12) are shown in Fig. 1. The calibration factor for the half-hourly negative and positive sensible heat flux density values were 0.728 and 0.325, respectively. The α value over the experimental sites ranged from 0.248 to 0.728 for the negative H values, and from 0.325 to 0.437 for the positive H values. Fig. 2 shows the least-squares regression through the origin of half-hourly SR-calibrated $\alpha H'$ versus the EC H from the E12 experiment. The calibrated SR $\alpha H'$ underestimated the EC H by less than 1% (Fig. 2), which indicates an excellent match of the two methods (Snyder et al. 1996; Spano et al. 2000).

Using the EC and SR estimates of H, latent heat flux density was calculate as the REB, using the same R_n and G, and a plot of the LE comparison is shown for the E12 rice field in Fig. 3. The REB estimates of LE calculated with EC and SR had a nearly 1:1 relationship with a high coefficient of determination $(R^2) = 0.99$, RMSE = 25 W m^{-2}, and NRMSE = 16% from a data set with $n = 4{,}576$. Similar results were found for the other experimental fields for all years; therefore, the LE values estimated from the SR analysis provide excellent estimates of LE for all of the research fields during the 2011–2013 experiments. Thus, the calibrated SR technique is a good independent method for estimating surface fluxes. Castellvi et al. (2006) also found reliable estimates of LE using SR analysis over rice.

There was a high correlation between the LE values and available energy ($R_n - G$) on both half-hourly and daily time scales. As

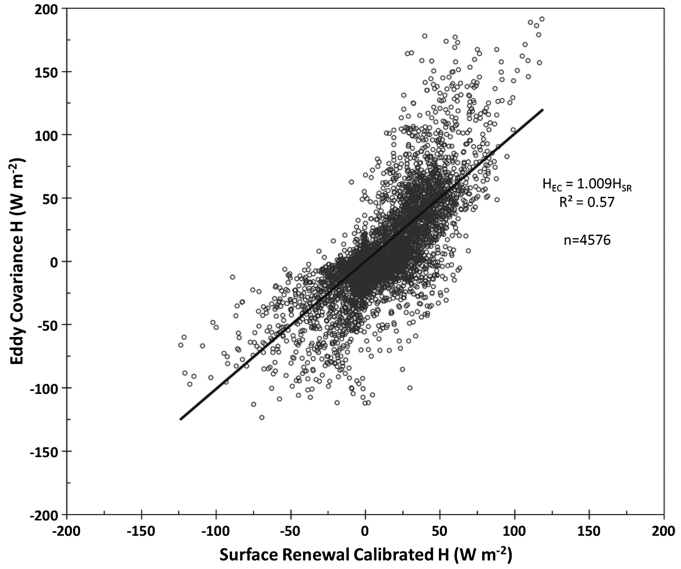

Fig. 2. Plot of the least-squares regression through the origin of half-hourly EC H versus calibrated SR $\alpha H'$ (E12 rice field)

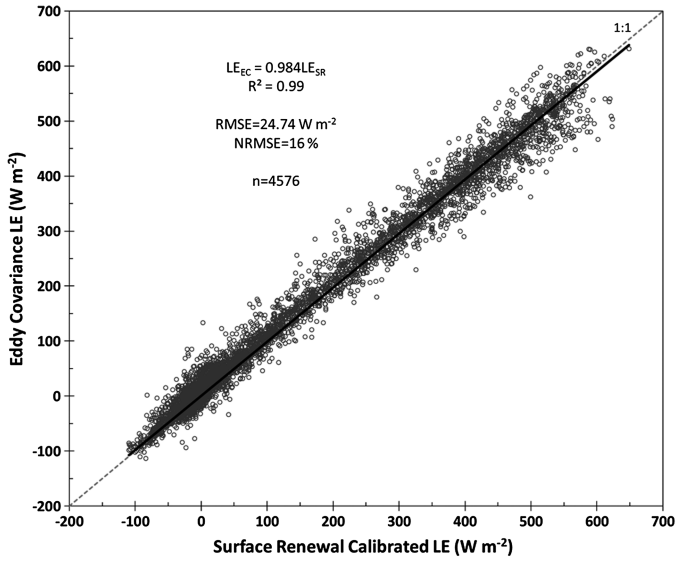

Fig. 3. Half-hourly EC LE versus calibrated SR LE for the E12 rice field, in which LE was calculated using the REB and either calibrated SR H or EC H

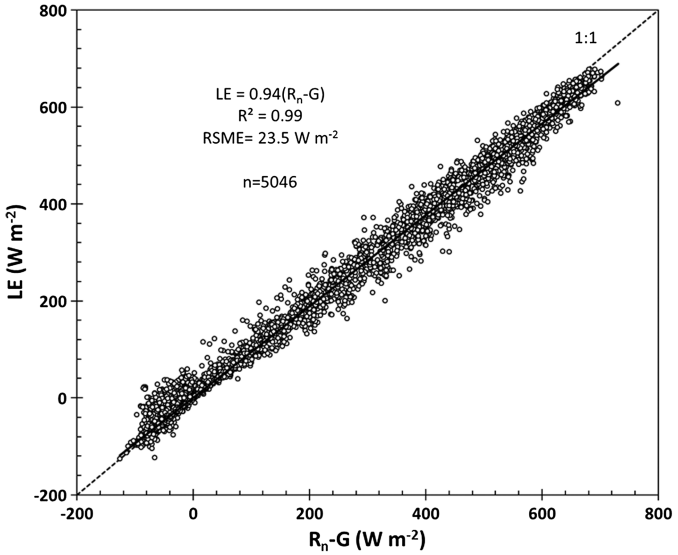

Fig. 4. Half-hourly SR estimated LE versus half-hourly $R_n - G$ for the N12 rice experiment

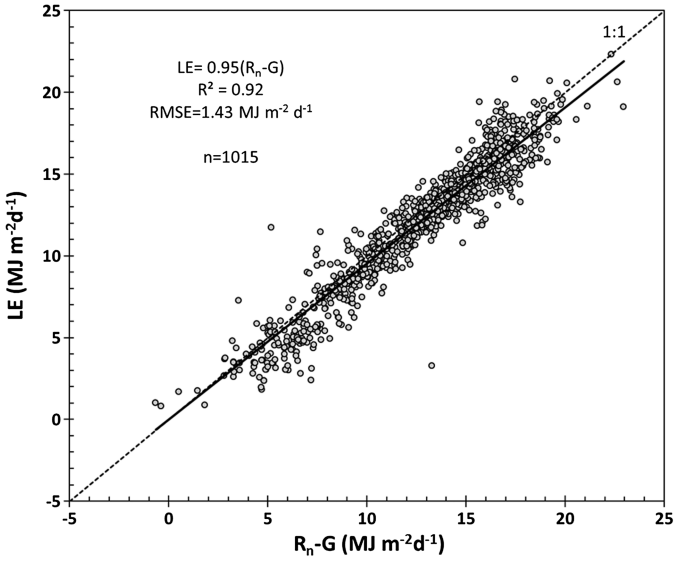

Fig. 5. Daily SR estimated LE versus daily $R_n - G$ from all experiments during 2011–2013

an example, the half-hourly data set of the LE versus $R_n - G$ for the experiment in the north rice field in 2012 (N12) is shown in Fig. 4. A plot of daily LE versus $R_n - G$ for all the experiments during 2011–2013 is presented in Fig. 5. The slope of the regression of the LE versus the $R_n - G$ through the origin was 0.94, and the R^2 was 0.99 for the half-hourly data set. The slope through the origin was 0.95 with $R^2 = 0.92$ for daily data. This implies that approximately 99% of the half-hourly LE can be explained by using the equation $LE = 0.94 \cdot (R_n - G)$ with a RMSE of 23.5 W m^{-2}. In addition, approximately 92% of the daily LE may be explained by using the equation $LE = 0.95 \cdot (R_n - G)$ with a RMSE of 1.43 MJ m^{-2} d^{-1}. The remainder of the variation in LE is likely the result of other factors (e.g., wind, air temperature, water temperature).

Daily Actual Evapotranspiration

One objective was to estimate the daily actual evapotranspiration (ET_a) of the crop using ET_o and crop coefficients. Because paddy rice is grown mostly in standing water, it was assumed that there is no water or salinity stress and ET_a is equal to the unstressed potential evapotranspiration (ET_c), in which daily $ET_c = ET_o \times K_c$ and K_c is a daily crop coefficient for potential ET of the crop. Evapotranspiration is measured by calculating half-hourly latent heat flux density as the REB using a calibrated SR value $\alpha H'$ for H [Eq. (3)]. The daily LE is derived as the sum of the 48 half-hourly LE calculations over a 24-h day. Daily LE (MJ m^{-2} d^{-1}) is converted to daily ET_c (kg m^{-2} d^{-1} or mm d^{-1}) using $ET_a = LE/2.45$, in which 2.45 MJ kg^{-1} is the latent heat of vaporization of water. Fig. 6 shows the observed rice ET_c and ET_o from spatial CIMIS from the different experimental fields.

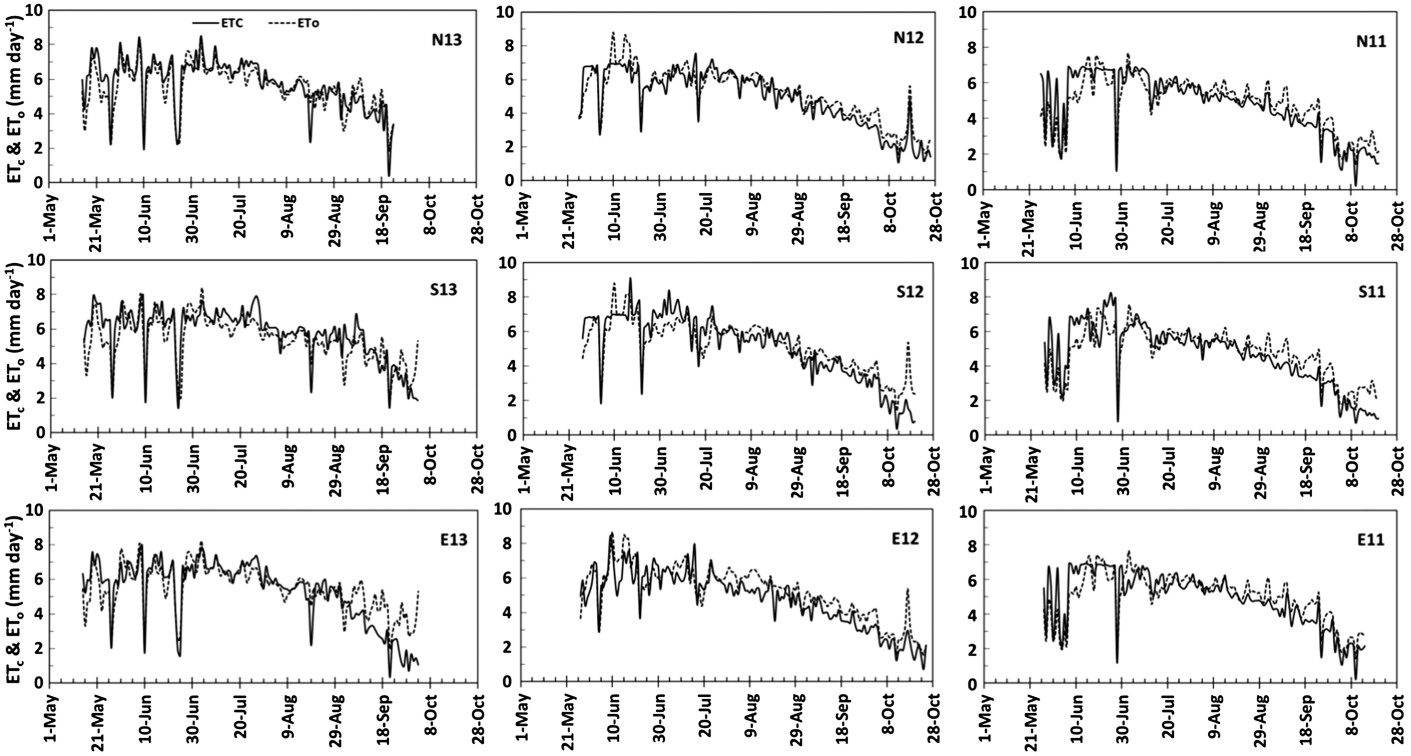

Fig. 6. Plots of ET_o and rice ET_c versus date by location (N = north, E = east, and S = south) and date (11 = 2011, 12 = 2012, and 13 = 2013); the rice field locations and seasons are identified in Table 1

Table 3. Mean, Maximum, and Minimum Daily ET_c and ET_o by the Experimental Fields, Identified by the Field Identification Number (Table 1) That Indicates the Location and Year

	ET_c (mm d^{-1})			ET_o (mm d^{-1})			
Field identifier number	Mean	Maximum	Minimum	Mean	Maximum	Minimum	Mean seasonal K_c (= ET_c/ET_o)
N11	4.8	7.0	0.2	4.8	7.7	1.4	1.00
N12	4.9	7.5	1.1	5.2	8.8	1.6	0.94
N13	5.8	8.5	0.4	5.6	8.4	1.9	1.03
S11	4.6	8.3	0.3	4.8	7.6	1.5	0.95
S12	5.1	9.1	0.4	5.2	8.8	1.4	0.98
S13	5.7	8.0	1.3	5.4	8.4	1.7	1.06
E11	4.9	6.9	0.2	5.0	7.7	1.4	0.98
E12	4.8	8.4	0.7	5.2	8.7	1.6	0.92
E13	5.3	8.0	0.3	5.5	8.2	2.0	0.96

The mean, maximum, and minimum daily ET_c and ET_o are given for each of the nine research fields in Table 3, and the mean daily ET_c was highest in 2013. The overall mean seasonal daily ET_c value was 5.1 mm d^{-1}. The highest maximum daily ET_c was observed in the south rice field during 2012 (9.1 mm d^{-1}), and the lowest minimum daily ET_c was found in the north and east rice fields during 2011 (0.2 mm d^{-1}).

Although there was no significant difference among the mean daily ET_c of the experimental fields within the same seasons, there were site differences in daily ET_c on some days. For example, on September 7, 2013, the daily ET_c of the north, east, and south sites were observed as 4.6, 4.0, and 6.9 mm d^{-1}, respectively. Thus, the daily ET_c of the north and east fields were 33 and 42% lower than the south rice field on that day. It is common to have strong wind speeds at the south but not necessarily at the north or east locations in the fall, so the large difference is not unexpected. According to the mean seasonal ET_c observed and the ET_o values from spatial CIMIS, the mean seasonal rice K_c for the experimental sites ranged from 0.92 to 1.06 (Table 3) for the M-206 rice variety in the Sacramento Valley. Comparisons of ET_c and ET_o at the experimental fields during the seasons revealed that the maximum values of the daily ET_o and ET_c were close, i.e., less than 10% differences. The difference between the minimum daily ET_c and ET_o ranged from 23 to 85%.

Growth Dates

To identify the ends of the growth periods for the K_c curve, the ratio R_n/R_s rather than ET_c/ET_o was used to remove variability from the data, to more easily identify the inflection points. The ratio R_n/R_s for rice was observed to change as the rice grew and senesced over the season. Because rice LE depends primarily on R_n, it is likely that both R_n and LE will change in a similar manner relative to R_s during the season. Using the plotted R_n/R_s data from

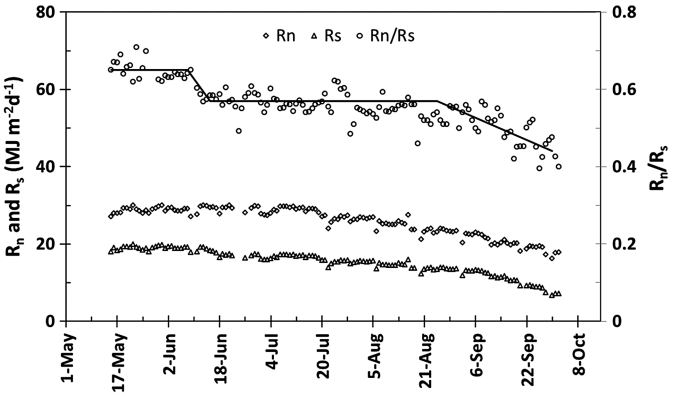

Fig. 7. Plots of daily solar radiation (R_s), net radiation (R_n), and the ratio R_n/R_s for data from the three rice fields studied in 2013; all of the fields were seeded on May 15 and two fields ended the season on October 2, with the third field ending on September 23

the three rice fields in 2013, the inflection points were determined subjectively as shown in Fig. 7. The inflection points were identified as A (May 15), B (June 9), C (June 17), D (September 1), and E (October 2). It is assumed that the inflection points based on R_n/R_s are the same as those for ET_c/ET_o.

After determining the dates for the inflection points, the percentages of the season from first flooding (Date A) to the end of initial growth (Date B), the end of rapid growth (Date C), and the end of midseason (Date D) were determined (Table 4). During the period from Date A to Date B, the field is mostly covered in water, and toward the end of this period, the rice plants start to emerge above the water surface. During Date B to Date C, the plants grow rapidly until canopy closure. Dates C to D cover the midseason period, which includes the season from late vegetative stage past heading. Date D occurs typically when the water is drained from the field and the plant leaves have started senescence (i.e., approximately 3 weeks after heading), and the late season from Date D to E is the period for final grain filling and drying. The K_c curve method in this study assumes that the percentages of the season from Date A to the ends of the various growth periods change little from year to year. The dates corresponding to various inflection points are determined easily for any input beginning and ending date using the percentages of the season to the various inflection dates. Therefore, using the percentage of the season approach helps irrigators to more easily identify their K_c curve from inputs of only Dates A and E.

Fig. 7 shows that the ratio R_n/R_s during initial growth from May 15 to June 9 is higher than for midseason and late season. Because net radiation is the main source of energy for ET_c, and it decreased as the canopy developed as a result of higher albedo from the crop canopy, the available energy for ET_c decreased as the canopy grew fast during the rapid growth period. The available energy also dropped dramatically during the late season, presumably because the surface was drying and heating after draining water from the fields.

Table 4. Dates Corresponding to the Ends of Growth Periods and Percentages of the Season from First Wetting (Date A) to the End of the Season (Date E)

Inflection point	Calendar date	Percentage of season
A	May 15	0
B	June 9	18
C	June 17	24
D	September 1	78
E	October 2	100

Rice Crop Coefficient

The observed daily K_c values and water levels for each paddy during the experiments are shown in Fig. 8. Using the dates corresponding to first flooding (Date A) and the end of the season (Date E) from each of the nine experimental fields, the percentages of the season from Table 4 were used to determine the calendar dates corresponding to end-point dates B, C, and D (Table 5). The optimal initial-growth K_{c1} (Dates A to B), midseason K_{c2} (Date C to D), and end-of-season K_{c3} (Date E) were determined by using trial and error to raise and lower the K_{c1}, K_{c2}, and K_{c3} values to find the smallest RMSE between the daily predicted and observed crop evapotranspiration over the season. Using this approach, an estimated K_c curve was derived for each of the nine fields. The growth dates for each experiment are given in Table 5, and the K_c curve that gave the best fit of $ET_{c(P)}$ with $ET_{c(O)}$ is plotted with the observed K_c values by rice field (Fig. 8). The calendar dates corresponding to growth period end dates are listed in Table 5.

The results indicate that there is considerable variability in rice water use, both spatially and temporally (Table 6). The average 3-year measured seasonal ET_c of the experimental fields during the 2011–2013 season ranged from 681 to 762 mm in Butte County (Fields N11, N12, N13, E11, E12, E13) and from 681 to 813 mm in the Williams, Colusa County (Fields S11, S12, S13). The mean seasonal ET_c of the rice paddies during 2011 to 2013 was 740 mm, which similar to the range of 700–800 reported by Spanu et al. (2009).

The RMSE and NRMSE values for a comparison of daily ET_c, which were predicted using the proposed K_c curve and observed ET_c for each of the experimental plots, are given in Table 6. Overall, the RMSE = 0.77 mm d^{-1} and NRMSE = 15% demonstrate good accuracy.

Discussion

Typical K_c Curve for Rice in the Sacramento Valley

According to all of the data during 2011–2013 at three experimental plots, the best-fit K_c values were 1.09 during initial growth, 0.99 during midseason, and 0.57 at Date E. Reporting K_c values to the nearest 0.01, however, is misleading because it implies much better accuracy in estimating ET than is possible. In FAO 24 and 56, K_c values are typically rounded to the nearest 0.05. Therefore, the values 1.10, 1.00, and 0.80 (average between the K_c values of Date D and Date E) were selected for use in the generalized K_c curve as the initial-growth, midseason, and late-season K_c values, respectively (Fig. 9).

The actual growth dates varied considerably from year to year in these studies. For M-206 rice crop grown in the Sacramento Valley, the season is approximately 145 days, and the typical growth dates are (A) May 1, (B) May 26, (C) June 4, (D) August 25, and (E) September 22. These dates are recommended by UC Farm Advisors and Specialists based on years of field observations. The corresponding percentages of the 145-day season are A–B (18%), A–C (24%), A–D (78%), and A–E (100%).

The daily ET_c observations for the all 2011–2013 seasons were evaluated against the daily ET_c values predicted from the proposed K_c model (Fig. 10). The daily ET_c that was predicted using ET_o and K_c values was plotted versus the observed ET_c, and a linear

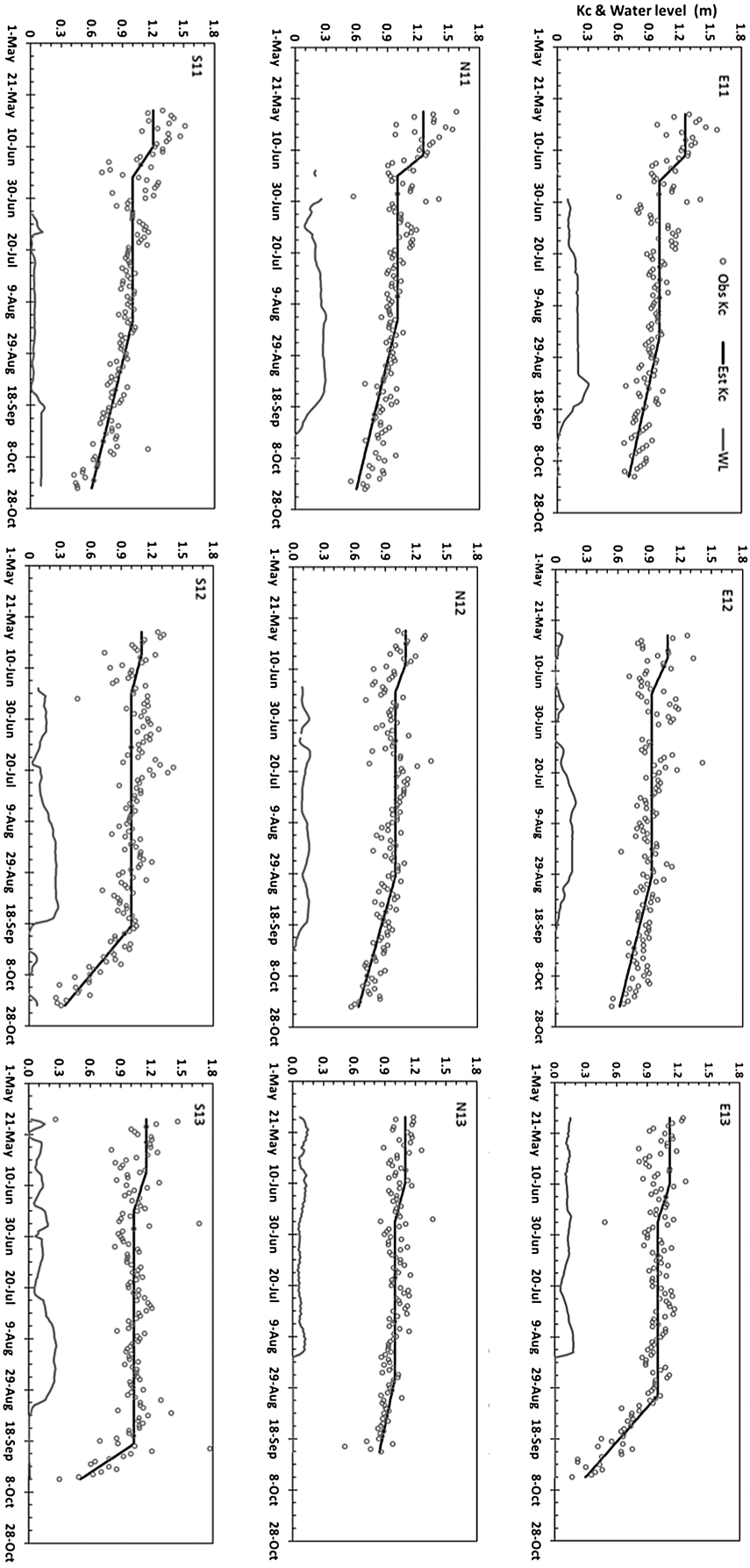

Fig. 8. Observed daily K_c values, predicted seasonal K_c curves, and daily water level at experimental fields, which are identified by location and year (Table 1); the calendar dates for the inflection points in the K_c curves are provided in Table 5

Table 5. Calendar Dates Corresponding to the End Points of the Growth Periods by Season

End points	A	B	C	D	E
% of season	0	18	24	78	100
N11	May 26	June 21	June 30	September 18	October 20
E11	May 27	June 21	June 29	September 13	October 14
S11	May 27	June 22	July 1	September 18	October 20
N12	May 26	June 22	July 1	September 23	October 26
E12	May 27	June 23	July 2	September 22	October 25
S12	May 27	June 22	July 1	September 18	October 20
N13	May 15	June 7	June 15	August 25	September 23
E13	May 15	June 9	June 18	September 2	October 3
S13	May 15	June 9	June 18	September 2	October 3

relationship $ET_{c(p)} = 1.02 \cdot ET_{c(o)}$ with $R^2 = 0.90$, RMSE of 0.58 mm d^{-1}, and NRMSE of 11.4% was found. Because the NRMSE = 11.4% is quite close to the 10% error expected for high-precision lysimeter measurements (W. O. Pruitt, personal communication), this comparison demonstrates that the prediction model of daily actual ET using ET_o and the developed K_c values is quite accurate.

Multiseasonal Rice Actual ET and K_c

The mean observed daily ET_c and K_c by month of each rice paddy experiment were calculated. The results for K_c values were plotted and the best-fit trendline-predicted monthly K_c values was illustrated in Fig. 11.

The maximum and minimum monthly ET_c values were 6.1 and 2.0 mm d^{-1}, respectively, and the mean seasonal daily ET_c of the area was 5.3 mm d^{-1}. Tabbal et al. (2002) reported typical ET_c rates of lowland rice fields of 4–5 mm d^{-1} in the wet seasons and 6–7 mm d^{-1} in the dry seasons, with values as high as 10–11 mm d^{-1} in subtropical regions. Because the ET_o rates were not reported in the Tabbal et al. (2002) study, it is not possible to make direct comparisons. For most areas in Asia, rice ET_c varies from 4–9 mm d^{-1} (Wickham and Sen 1978). In a tropical dry season, De Datta (1981) reported a common daily rice ET_c rate of 6–7 mm d^{-1}.

Spanu et al. (2009) reported mean daily midseason ET_c of 5.8 mm d^{-1} for Mediterranean conditions in Italy, which was 5% higher than the mean rate proposed by Abdullahi et al. (2013). Moratiel and Martínez-Cob (2013) reported 5.2 mm d^{-1} as the average daily ET_c for midseason of sprinkler-irrigated rice in a semiarid region of Spain.

For these experiments, the monthly mean K_c values varied from 0.72 in October to 1.16 during initial growth in May. A trendline using Eq. (5) is shown in Fig. 11 for mean K_c versus month (with $R^2 = 0.99$). Clearly, the trendline shows a good relationship between K_c versus month of the year

$$K_c = -0.0055(\text{MoY})^3 + 0.1155(\text{MoY})^2 - 0.8529(\text{MoY}) + 3.2171 \quad (5)$$

where MoY = month number, between 5 and 10.

Fig. 12 illustrates a stage-wise comparison of average rice K_c values obtained in the present study with the respective K_c values reported by other researchers. In the initial-growth period, the proposed K_c value in this work is 15% higher than the corresponding K_c value given by others, except for the K_c value recommended by Tyagi et al. (2000), which is 4% lower. Based on the observed net radiation, which was considerably higher during initial growth than during other periods, and the fact that the net radiation sensors are much improved in this study over those available in the past, it is likely that the initial growth ET_c was underestimated in past experiments. The experiment by Moratiel et al. (2013) used improved net radiometers, but their experiment was over upland and not paddy rice, so they did not observe an elevated R_n during initial growth.

An obvious K_c difference was found during the midseason growth period. Because midseason occurs when ET_o rates are highest, accurate K_c values are critically important. The midseason K_c value found in this study is lower than the K_c values reported by

Table 6. Days in the Season, Observed Cumulative Total ET_c, RMSE, and NRMSE Values for a Comparison of Daily Predicted ET_c and Observed ET_c by Experimental Plot

Experimental plot	E11	E12	E13	N11	N12	N13	S11	S12	S13
Days in the season	141	152	142	148	154	132	147	147	142
Seasonal observed ET_c (mm)	690	726	759	711	759	762	681	757	813
RMSE (mm d^{-1})	0.68	0.87	0.79	0.65	0.70	0.70	0.75	0.75	0.99
NRMSE (%)	15	18	17	14	14	13	17	15	19

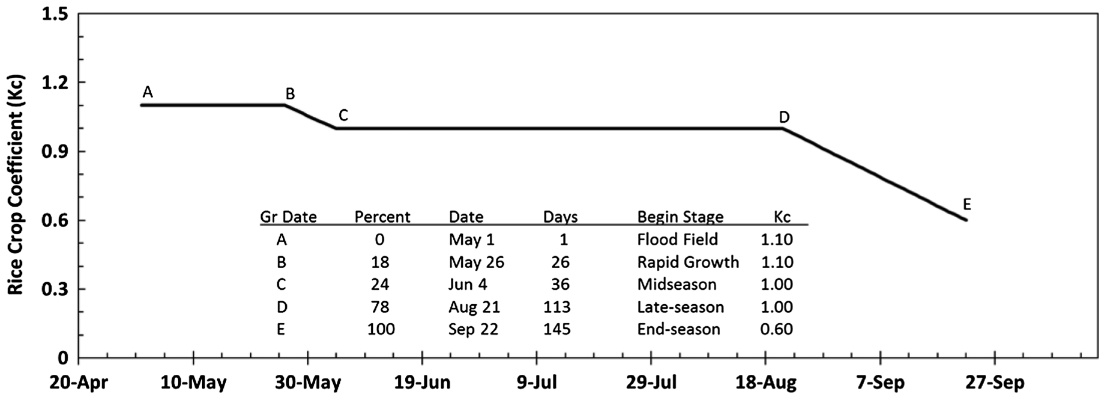

Fig. 9. Typical K_c curve for rice, M-206 variety, in the Sacramento Valley

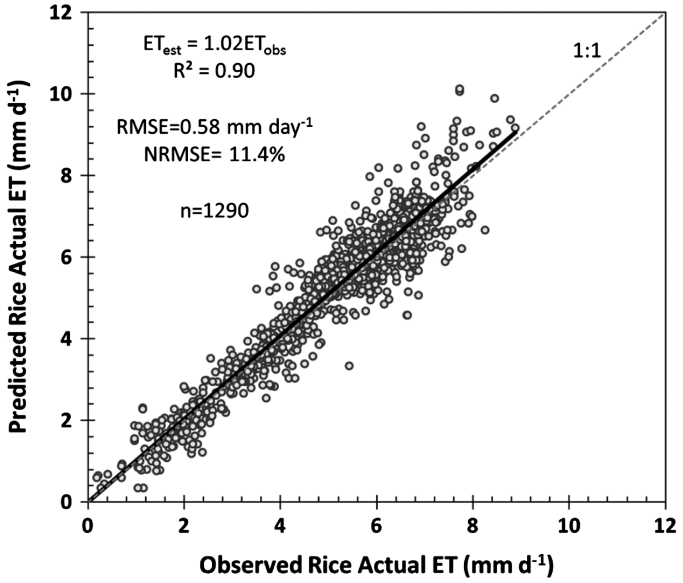

Fig. 10. Predicted ET versus observed ET during 2011–2013

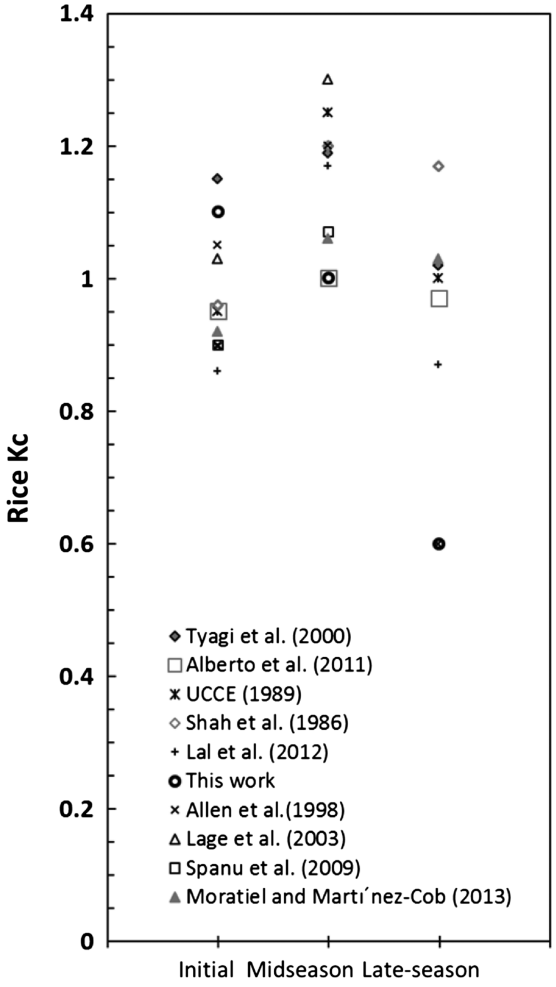

Fig. 12. Comparison of rice K_c values during initial growth, midseason, and late season

others (averaging 13% lower). The midseason K_c value reported in this study is the same as that obtained by Alberto (2011), and is 16% lower than the value recommended by Allen et al. (1998). The reported K_c values for both initial-growth and midseason stages are also similar to the 1.02–1.05 obtained by Lourence and Pruitt (1971). The K_c value for late season is approximately 20% less than the values presented by the other studies, with a K_c 33% higher than the value recommended by Allen et al. (1998).

The derived crop coefficients differed from some of the K_c values reported in the literature. This difference may be attributed to the changes in climatic conditions, variety, management practices, length of growing season, crop canopy height, ground cover percentage, field measurement techniques, and the methodology to calculate ET_o. Although the paddy rice K_c may also change over time at the same location, the temporal and spatial variations need to be considered. Because the ratio of net radiation to solar radiation during the early-season stage at the rice paddy fields was 12% higher than the corresponding ratio during midseason (Fig. 7), it appears that much of the difference between this research and earlier studies is related to the net radiation measurements. In general, flooded rice paddies, with minimal vegetation, had lower albedo, and the albedo increased as the rice plants grew and covered the surface. Sensible heat flux density was consistently near zero at all hours of the day during the initial growth, primarily because there was little turbulence over the flat water surface. As the canopy developed, the turbulence and sensible heat flux increased, which led to positive upward H after sunrise and negative H from about noon through the following morning. Approximately 95% of the latent heat flux density can be explained as a linear function of $R_n - G$ during the season (Fig. 5).

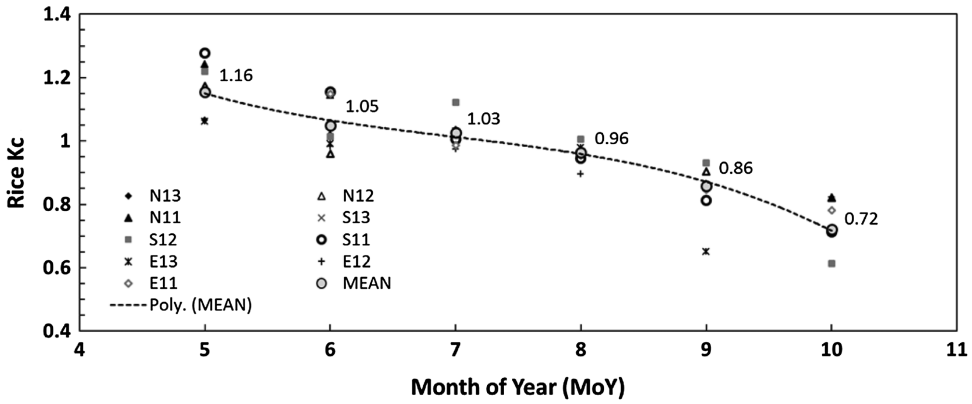

Fig. 11. Monthly means of daily rice K_c values versus month and a trendline; see Eq. (5) for the trendline equation

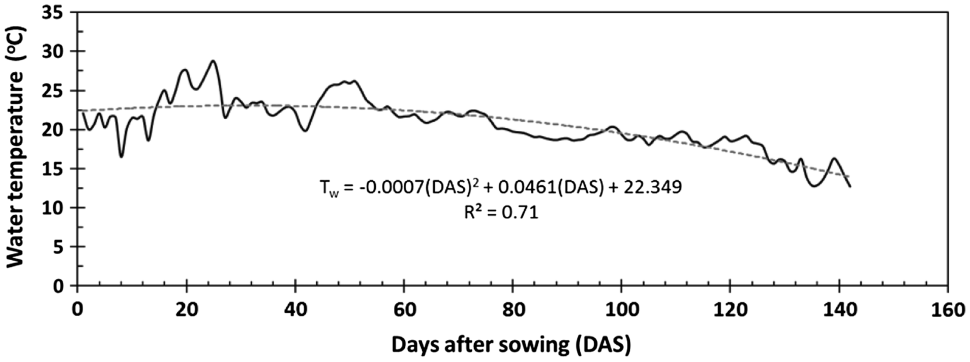

Fig. 13. Seasonal mean daily water temperature in the east rice paddy during 2013 (E13)

The mean daily water temperature within the paddy fields decreased throughout the season after sowing. For example, Fig. 13 shows the average daily water temperatures within the east experimental paddy during the 2013 season. The early season variation was most likely the result of changes in early-season cloud cover. The skies are mostly clear from mid-June to September, and the decrease in water temperature is mostly the result of the plant canopy shading the water from solar radiation. The mean daily water temperature within the E13 experimental paddy was clearly lower during midseason (from 36 to 113 DAS) than during early season. The same trend was obtained over all of the experiments. Thus, the higher K_c during early season is probably partly the result of higher water temperature. In the directly seeded systems in California, during the first 2–3 weeks of the season, the plant canopy is a relatively minor part of the system. The planting system clearly has an effect on the energy balance components, and it helps to explain the unusual shape of the seasonal K_c curve (Fig. 9).

Conclusions

Precise ET_o monitoring and application of more accurate growth stage-specific K_c provide a basic tool for determining water balance information to assist growers at optimizing irrigation management. In the present study, the actual rice ET_c was measured and a typical K_c curve was developed for the Sacramento Valley in California using the residual of the energy balance method over three paddy rice fields during three growing seasons. The developed K_c curve should work well for a comparable rice variety in any location having a climate similar to the California Sacramento Valley. Although windy conditions are uncommon in the Sacramento Valley, higher K_c values might be expected in a windier climate.

There was a high correlation between the ET_c and available energy, i.e., net radiation minus water and ground heat storage, on both an hourly and a daily time scale. Net radiation decreased as the canopy developed, because of higher albedo from the rice canopy than from the flooded field. The rice K_c values were lower than those commonly used to estimate rice ET_c during the midseason, and were higher than expected during early growth before canopy closure. The ability and accuracy of the generalized K_c curve were evaluated and found to be adequate for practical application. The proposed monthly K_c curve enables growers to determine rice crop water use in a reliable, usable, and affordable format. The derived K_c information, along with current and projected ET_o estimates, provides rice ET_c data for planning agricultural water demand and for water transfers to water-short areas of the State.

Acknowledgments

The authors thank the California Department of Water Resources for supporting the "Refinement of Rice Water Use" project, Agreement No. 460008548A12TOUC101. The authors especially thank Tom Filler and Al Vargas from the Water Transfer Office and Morteza Orang and Tom Hawkins from the Water Planning Office for their valuable input and feedback during the project.

References

Abdullahi, A. S., Mohammad Soom, A. A., Ahmad, D., and Mohamed Shariff, A. R. (2013). "Characterization of rice (*Oryza sativa*) evapotranspiration using micro paddy lysimeter and class "A" pan in tropical environments." *Aust. J. Crop Sci.*, 7(5), 650–658.

Aguilar, M., and Borjas, F. (2005). "Water use in three rice flooding management systems under Mediterranean climatic conditions." *Spanish J. Agric. Res.*, 3(3), 344–351.

Alberto, M. C., et al. (2011). "Comparisons of energy balance and evapotranspiration between flooded and aerobic rice fields in the Philippines." *Agric. Water Manage.* 98(9), 1417–1430.

Alberto, M. R., et al. (2011). "Comparisons of energy balance and evapotranspiration between flooded and aerobic rice fields in the Philippines." *Agric. Water Manage.*, 98(9), 1417–1430.

Allen, R. G., Pereira, L. S., Howell, T. A., and Jensen, M. E. (2011). "Evapotranspiration information reporting. I: Factors governing measurement accuracy." *Agric. Water Manage.*, 98(6), 899–920.

Allen, R. G., Pereira, L. S., Raes, D., and Smith, M. (1998). "Crop evapotranspiration: Guidelines for computing crop water requirements." Food and Agricultural Organization of the United Nations (FAO), Rome.

Anandakumar, K. (1999). "Sensible heat flux over a wheat canopy: Optical scintillometer measurements and surface renewal analysis estimations." *Agric. For. Meteorol.*, 96(1–3), 145–156.

California Department of Water Resources. (1998). "Statewide agricultural land and water use estimates database." Sacramento, CA.

Castellví, F., Consoli, S., and Papa, R. (2012). "Sensible heat flux estimates using two different methods based on surface renewal analysis: A study case over an orange orchard in Sicily." *Agric. For. Meteorol.*, 152(1), 58–64.

Castellví, F., and Snyder, R. L. (2009). "On the performance of surface renewal analysis to estimate sensible heat flux over two growing rice fields under the influence of regional advection." *J. Hydrol.*, 375(3–4), 546–553.

Castellví, F., and Snyder, R. L. (2010). "A new procedure based on surface renewal analysis to estimate sensible heat flux: A case study over grapevines." *J. Hydrometeorol.*, 11(2), 496–508.

Castellví, F., Snyder, R. L., and Baldocchi, D. D. (2008). "Surface energy-balance closure over rangeland grass using the eddy covariance method and surface renewal analysis." *Agric. For. Meteorol.*, 148(6–7), 1147–1160.

Castellví, F., Snyder, R. L., Baldocchi, D. D., and Martínez-Cob, A. (2006). "A comparison of new and existing equations for estimating sensible heat flux using surface renewal and similarity concepts." *Water Resour. Res.*, 42(8), 1–18.

Chahal, G. S., Sood, A., Jalota, S. K., Choudhury, B. U., and Sharma, P. K. (2007). "Yield, evapotranspiration and water productivity of rice (*Oryza sativa* L.)-wheat (*Triticun aestivum* L.) system in Punjab (India) as influenced by transplanting date of rice and weather parameters." *Agric. Water Manage.*, 88(1–3), 14–22.

Consoli, S., O'Connell, N. V., and Snyder, R. L. (2005). "Estimation of evapotranspiration of different sized navel orange-tree orchards using energy balance." *J. Irrig. Drain. Eng.*, 061/(ASCE)0733-9437(2006) 132, 2–8.

De Datta, S. K. (1981). *Principles and practices of rice production*, International Rice Research Institute, Los Baños, Phillippines.

Doorenbos, J., and Pruitt, W. O. (1977). "Crop water requirements." FAO, Rome.

Drexler, J. Z., Anderson, F. E., and Snyder, R. L. (2008). "Evapotranspiration rates and crop coefficients for a restored marsh in the Sacramento-San Joaquin Delta, California, USA." *Hydrol. Processes*, 22(6), 725–735.

FAO (Food and Agriculture Organization of the United Nations). (1977). *Guidelines for predicting crop water requirements*, J. Doorenbos and W. O. Pruitt, eds., Rome.

Hart, Q. J., Brugnach, M., Temesgen, B., Rueda, C., Ustin, S. L., and Frame, K. (2009). "Daily reference evapotranspiration for California using satellite imagery and weather station measurement interpolation." *Civ. Eng. Environ. Syst.* 26(1), 19–33.

Lage, M., Bamouh, A., Karrou, M., and El Mourid, M. (2003). "Estimation of rice evapotranspiraton using a rice microlysimeter technique and comparison with FAO Penman-Monteith and Pan evaporation methods under Moroccan conditions." *Agronomie*, 23(7), 625–631.

Lal, D., Clark, B., Bettner, T., Thoreson, B., and Snyder, R. L. (2012). "Rice evapotranspiration estimates and crop coefficients in Glenn-Colusa irrigation district, Sacramento Valley, California." *Proc., USCID Water Management Conf.*, USCID, Denver.

Lee, X., Massman, W. J., and Law, B. E. (2004). *Handbook of micrometeorology: A guide for surface flux measurement and analysis*, Kluwer, London.

Linquist, B., et al. (2015). "Water balances and evapotranspiration in water- and dry-seeded rice systems." *Irrig. Sci*, 33, 375–385.

Lourence, F. J., and Pruitt, W. O. (1971). "Energy balance and water use of rice grown in the central valley of California." *Agron. J.*, 63(6), 827–832.

Massman, W. J., and Lee, X. (2002). "Eddy covariance flux corrections and uncertainties in long-term studies of carbon and energy exchanges." *Agric. For. Meteorol.*, 113(1–4), 121–144.

Mohan, S., and Arumugam, N. (1994). "Irrigation crop coefficients for lowland rice." *Irrig. Drain. Syst.*, 8(3), 159–176.

Moratiel, R., and Martínez-Cob, A. (2012). "Evapotranspiration of grapevine trained to gable trellis system under netting and black plastic mulching." *Irrig. Sci.*, 30(3), 167–178.

Moratiel, R., and Martínez-Cob, A. (2013). "Evapotranspiration and crop coefficients of rice (*Oryza sativa* L.) under sprinkler irrigation in a semiarid climate determined by the surface renewal method." *Irrig. Sci.*, 31(3), 411–422.

Paw U, K. T., and Brunet, Y. (1991). "A surface renewal measure of sensible heat flux density." *Proc., 20th Conf. on Agriculture and Forest Meteorology*, American Meteorological Society, Boston, 52–53.

Paw U, K. T., Qiu, J., Su, H. B., Watanabe, T., and Brunet, Y. (1995). "Surface renewal analysis: A new method to obtain scalar fluxes without velocity data." *Agric. For. Meteorol.*, 74(1–2), 119–137.

Paw U, K. T., Snyder, R. L., Spano, D., and Su, H. B. (2005). "Surface renewal estimates of scalar exchange." *Micrometeorology in agricultural systems*, J. L. Hatfield and J. M. Baker, eds., Agronomy Society of America, Madison, WI, 455–483.

Reuss, J. O. (1980). "Matching cropping systems to water supply using an integrative model." *Water Management Technical Rep. 62*, Water Management Research Project, Colorado State Univ., Fort Collins, CO.

Rosa, R., Dicken, U., and Tanny, J. (2013). "Estimating evapotranspiration from processing tomato using the surface renewal technique." *Biosyst. Eng.*, 114(4), 406–413.

Seung Hwan, Y., Jin-Yong, C., and Min Won, J. (2006). "Estimation of paddy rice crop coefficients for Penman-Monteith and FAO modified Penman method." *ASABE Annual Int. Meeting*, ASABE, St. Joseph, MI.

Shah, M. H., Bhatti, M. A., and Jensen, J. R. (1986). "Crop coefficients over a rice field in the central plain of Thailand." *Field Crops Res.*, 13, 251–256.

Shapland, T. M., McElrone, A. J., Paw U, K. T., and Snyder, R. L. (2013). "A turnkey data logger program for field-scale energy flux density measurements using eddy covariance and surface renewal." *Ital. J. Agrometeorol.*, 1, 1–9.

Shapland, T. M., McElrone, A. J., Snyder, R. L., and Paw U, K. T. (2012a). "Structure function analysis of two-scale scalar ramps. II: Ramp characteristics and surface renewal flux estimation." *Boundary Layer Meteorol.*, 145(1), 27–44.

Shapland, T. M., Snyder, R. L., Paw U, K. T., and McElrone, A. J. (2014). "Thermocouple frequency response compensation leads to convergence of the surface renewal alpha calibration." *Agric. For. Meteorol.*, 189–190, 36–47.

Shapland, T. M., Snyder, R. L., Smart, D. R., and Williams, L. E. (2012b). "Estimation of actual evapotranspiration in wine grape vineyards located on hillside terrain using surface renewal analysis." *Irrig. Sci.*, 30(6), 471–484.

Shaw, R. H., and Snyder, R. L. (2003). "Evaporation and eddy covariance." *Encyclopedia of water science*, B. A. Stewart and T. Howell, eds., Marcel Dekker, New York.

Snyder, R. L., and O'Connell, N. V. (2007). "Crop coefficients for microsprinkler irrigated, clean-cultivated, mature citrus in an arid climate." *J. Irrig. Drain. Eng.*, 10.1061/(ASCE)0733-9437(2007)133:1(43), 43–52.

Snyder, R. L., Pedras, C., Montazar, A., Henry, J. M., and Ackley, D. A. (2015). "Advances in ET-based landscape irrigation management." *Agric. Water Manage.*, 147(1), 187–197.

Snyder, R. L., and Pruitt, W. O. (1992). "Evapotranspiration data management in California." *Proc., Water Forum 92*, Baltimore.

Snyder, R. L., Spano, D., Duce, P., Paw U, K. T., and Rivera, M. (2008). "Surface renewal estimation of pasture evapotranspiration." *J. Irrig. Drain. Eng.*, 10.1061/(ASCE)0733-9437(2008)134:6(716), 716–721.

Snyder, R. L., Spano, D., and Paw U, K. T. (1996). "Surface Renewal analysis for sensible and latent heat flux density." *Boundary Layer Meteorol.*, 77(3–4), 249–266.

Spano, D., Snyder, R. L., Duce, P., and Paw U, K. T. (1997). "Surface renewal analysis for sensible heat flux density using structure functions." *Agric. For. Meteorol.*, 86(3–4), 259–271.

Spano, D., Snyder, R. L., Duce, P., and Paw U, K. T. (2000). "Estimating sensible and latent heat flux densities from grapevine canopies using surface renewal." *Agric. For. Meteorol.*, 104(3), 171–183.

Spanu, A, Murtas, A., and Ballone, F. (2009). "Water use and crop coefficients in sprinkler irrigated rice." *Ital. J. Agron.*, 4(2), 47–58.

Suvočarev, K., Blanco, O., Faci, J. M., Medina, E. T., and Martinez-Cob, A. (2013). "Transpiration of table grape (*Vitis vinifera* L.) trained on an overhead trellis system under netting." *Irrig. Sci.*, 31(6), 1289–1302.

Tabbal, D. F., Bouman, B. M., Bhuiyan, S. I., Sibayan, E. B., and Sattar, M. A. (2002). "On-farm strategies for reducing water input in irrigated rice: Case studies in the Philippines." *Agric. Water Manage.*, 56(2), 93–112.

Tsay, R. S. (2005). *Analysis of financial time series (Wiley series in probability and statistics)*, 2nd Ed., Wiley, Hoboken, NJ.

Tyagi, N. K., Sharma, D. K., and Luthra, S. K. (2000). "Determination of evapotranspiration and crop coefficients of rice and sunflower with lysimeter." *Agric. Water Manage.*, 45(1), 41–54.

UCCE (University of California Cooperative Extension). (1989). "Using reference evapotranspiration (ETo) and crop coefficients to estimate crop evapotranspiration (ETc) for agronomic crops, grasses and vegetable crops." Univ. of California, Berkeley, CA.

USDA. (2011). *2009 California rice county estimates*, ⟨http://www.nass.usda.gov/Statistics_by_State/California/Publications/County_Estimates/201006ricep.pdf⟩ (Oct. 31, 2011).

Van Atta, C. W. (1977). "Effect of coherent structures on structure functions of temperature in the atmospheric boundary layer." *Arch. Mech.*, 29, 161–171.

Webb, E. K., Pearman, G. I., and Leuning, R. (1980). "Correction of flux measurements for density effects due to heat and water vapor transfer." *Q. J. R. Meteorol. Soc.*, 106(447), 85–100.

Wickham, T. H., and Sen, C. N. (1978). "Water management for lowland rice: water requirements and yield response." *Soils and rice*, IRRI, Los Bafios, Philippines, 649–668.

Zapata, N., and Martínez-Cob, A. (2002). "Evaluation of the surface renewal method to estimate wheat evapotranspiration." *Agric. Water Manage.*, 55(2), 141–157.